Capillarity

Vol. 5, No. 4, p. 75-82, 2022

Original article

Stability analysis of the water bridge in organic shale nanopores: A molecular dynamic study

Jie Liu, Tao Zhang*, Shuyu Sun*

Physical Science and Engineering Division (PSE), Computational Transport Phenomena Laboratory, King Abdullah University of Science and Technology (KAUST), Thuwal 23955-6900, Saudi Arabia

Keywords:
Molecular dynamics
kerogen
water bridge
shale gas

Cited as:
Liu, J., Zhang, T., Sun, S. Stability analysis of the water bridge in organic shale nanopores: A molecular dynamic study. Capillarity, 2022, 5(4): 75-82.
https://doi.org/10.46690/capi.2022.04.02

Abstract:
In the last decades, shale gas development has relieved the global energy crisis and slowed global warming problems. The water bridge plays an important role in the process of shale gas diffusion, but the stability of the water bridge in the shale nanochannel has not been revealed. In this work, the molecular dynamics method is applied to study the interaction between shale gas and water bridge, and the stability can be tested accordingly. CO_2 can diffuse into the liquid H_2O phase, but CH_4 only diffuses at the boundary of the H_2O phase. Due to the polarity of H_2O molecules, the water bridge presents the wetting condition according to model snapshots and one-dimensional analyses, but the main body of the water bridge in the two-dimensional contour shows the non-wetting condition, which is reasonable. Due to the effect of the molecular polarity, CO_2 prefers to diffuse into kerogen matrixes and the bulk phase of water bridge. In the bulk of the water bridge, where the interaction is weaker, CO_2 has a lower energy state, implies that it has a good solubility in the liquid H_2O phase. Higher temperature does not facilitate the diffusion of CO_2 molecules, and higher pressure brings more CO_2 molecules and enhances the solubility of CO_2 in the H_2O phase, in addition, a larger ratio of CO_2 increases its content, which does the same effects with higher pressures. The stability of the water bridge is disturbed by diffused CO_2, and its waist is the weakest position by the potential energy distribution.

1. Introduction

In the past decades, the development of shale gas has drawn attention globally, which has been considered relatively clean energy compared with coal and petroleum (Zhang et al., 2019; Zhao et al., 2022). The shale reservoir is always associated with H_2O condition, and the bridge formed by H_2O in the micro pores plays an important role in the diffusion process (Shen et al., 2019; Huai et al., 2020), thus the stability of the water bridge is necessary to be studied in the understanding of shale gas development.

Shale reservoirs have extremely low permeability and porosity, and the pose size ranges from several nanometers to hundreds of micrometers (Javadpour, 2009; Liu et al., 2022b). By using the micro-Computed Tomography method, the micro fluid behaviors can be visualized (Yang et al., 2020a), but it is pretty hard to study the interactions between shale gas and the H_2O phase at the nanoscale. molecular dynamics (MD) method, which is based on the Newtonian mechanics, has been approved as an effective and accurate tool to study the adsorption and flow behaviors of shale fluid (Yang et al., 2017; Feng et al., 2020; Cui et al., 2022; Liu et al., 2022d), and the energy parameters of atoms can be evaluated precisely. The shale rock is mainly composed of organic and inorganic matters, and the organic matter is commonly distributed in the shale nanopores because of the blocked property of the shale reservoir, where kerogen is the main component of organic (Hunt and Jamieson, 1956; Rexer et al., 2014). Ungerer et al. (2015) constructed the molecular structure of kerogen

Yandy Scientific Press

*Corresponding author.
E-mail address: jie.liu.1@kaust.edu.sa (J. Liu); tao.zhang.1@kaust.edu.sa (T. Zhang); shuyu.sun@kaust.edu.sa (S. Sun).

2207-9963 © The Author(s) 2022.
Received July 2, 2022; revised July 23, 2022; accepted August 10, 2022; available online August 13, 2022.

monomers at different maturity. Perez and Devegowda (2019) studied the multicomponent fluid in the nanopores of kerogen matrix, and they found that the H_2O component tended to adsorb on the kerogen surface, while the CH_4 component preferred to enrich in the bulk pore space. However, the stability of water bridge in the condition of shale gas has not been studied.

Carbon capture, utilization, and storage (CCUS) is always a hot research point in the past fewer years (Kadoura et al., 2016; Zhou et al., 2019a; Zhang et al., 2020; An et al., 2021), and CO_2 flooding is an effective way to handle large amounts of CO_2 in the development of oil and gas (Liu et al., 2019; Yang et al., 2020c). Hence, the effects of shale gas mixed with CO_2 on the water bridge are necessary to be studied. Liu et al. (2022c) studied H_2O behaviors on the oil transport by using MD simulations, and the results presented that the water bridge would form with the effects of the channel confinement, which would inhibit the fluid flow. The capillarity forces caused by the water bridge in the clay pore impacted the fluid flow, and the capillarity force would vanish once the water bridge is broken (Ho and Striolo, 2015). CO_2 has also been confirmed that can break through the water bridge in shale nano channels, and improve the recovery of oil (Liu et al., 2022a). Aspenes et al. (2008) imaged the water bridge in the micro channel, and they concluded that the separate water bridge was stable in the experimental time scale. The effects of CO_2 on the stability of water bridge are still lacking. Hence, the stability of the water bridge is critical for the development of shale energy.

In this work, the MD method is applied to study the stability problem of water bridges in the kerogen channel, and the effects of CH_4 and CO_2 are also examined. The realistic kerogen monomers are adopted to build the organic nanopore, and the one-dimensional density distribution is analyzed. To present the interactive behaviors more clearly, the two-dimensional contours of density and potential energy are discussed. The sensitivities, which contain the temperature, pressure, and molar ratio, are also tested to verify the analyses in various conditions.

2. Methodology

2.1 Molecular models

The type II-D kerogen monomer was used to build the realistic organic channel (Ungerer et al., 2015), because it was commonly found in shale reservoirs. Forty-two kerogen monomers were filled in the simulation box, and the density of the kerogen matrix was kept at 1.1-1.2 g·cm^{-3} (Tesson and Firoozabadi, 2018). The construction process of kerogen matrix is same as our previous study (Liu et al., 2022d). The box size was 12.55 × 8.15 × 6.28 nm^3, and the thickness of the water bridge was 3 nm. The pore space was also filled with CH_4 and CO_2 molecules. After that, the molecular model was constructed, as shown in Fig. 1. The water bridge was built in the center of the kerogen slit, and its width was controlled at 3 nm to have a better quantitative analysis, because the water bridge with a larger or smaller width is good at showing the stable results. The visual molecular dynamics package is applied for visualization (Humphrey et al., 1996).

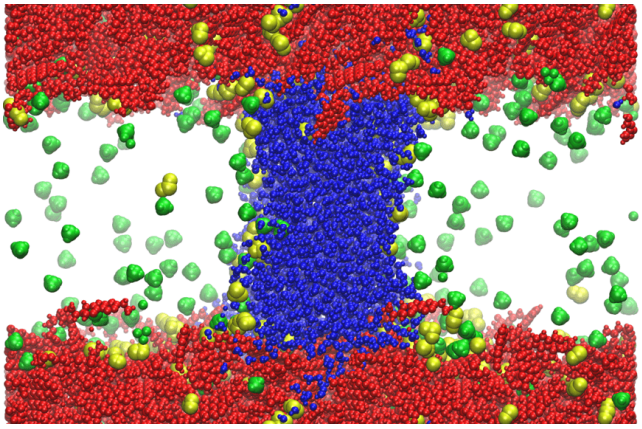

Fig. 1. Molecular models of the kerogen channel (red), water bridge (blue), CH_4 (green), and CO_2 (yellow).

All atoms in this model were applied with the parameters in the polymer consistent force field plus, which had been approved useful in the applications of kerogen models (Collell et al., 2014; Liu et al., 2020; Yang et al., 2020b), and the parameters between different atoms were calculated by Waldman-Hagler combining rules (Waldman and Hagler, 1993). The electrostatic interaction was controlled by the Ewald method (York et al., 1993), and the Van der Waals interaction was handled by the Lennard-Jones equation. The periodic condition was applied in all directions, and the cutoff distance was 1.2 nm.

2.2 Molecular dynamic simulations

The large-scale atomic/molecular massively parallel simulator package was used to carry out MD simulations (Srinivasan et al., 1997). Firstly, an constant-pressure, constant-temperature ensemble simulation was calculated for 100 ps with a timestep of 0.1 fs. After that, the canonical ensemble was presented for 1.5 ns with a timestep of 1 fs, and the trajectory was collected every 0.5 ns for the analysis. The kerogen matrix was frozen during the simulation to keep its stability. To reduce the randomness of the results, the simulations were calculated three times independently.

3. Results and discussion

In this section, the density analysis is presented to verify the effects of CH_4 and CO_2. The potential energy contours are carried out to study the water bridge on the mechanism level, which provides a better understanding of the stability of the water bridge in shale reservoirs. The effects of temperature, pressure, and the ratio of CH_4 and CO_2 are also examined.

3.1 Spatial distribution of CH_4 and CO_2

The density profiles of the water bridge and gas-phase molecules are counted by chunking the simulation box, and the density profiles are depicted in two directions, i.e., perpendicular to the water bridge and parallel to the water bridge, as shown in Fig. 1. As can be seen in Fig. 2(a), the density profiles of H_2O and CH_4 show the mixed boundary, because of the effect of molecular diffusion. Thus, the sharp interface between H_2O and CH_4 cannot be observed, which corresponds

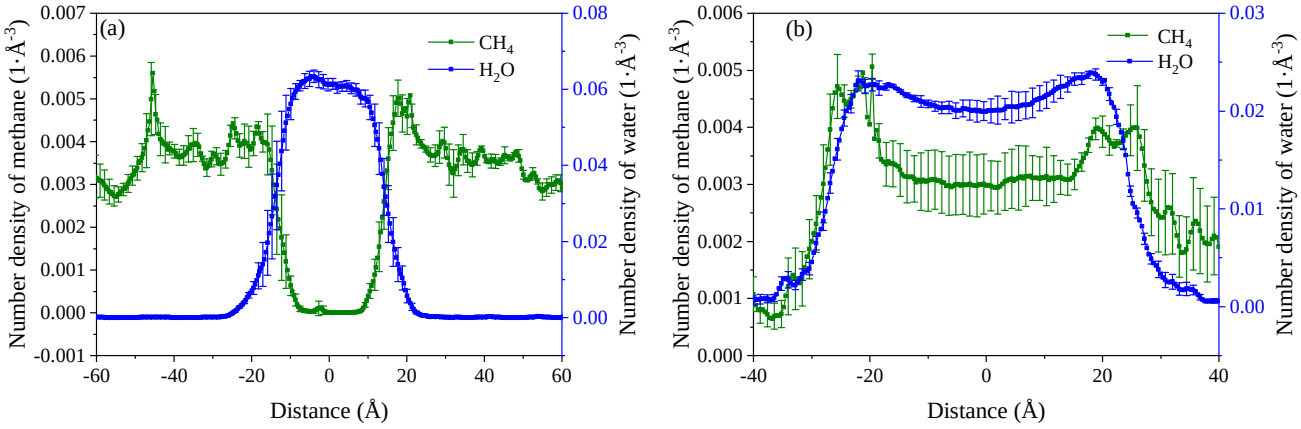

Fig. 2. The density profiles of the water bridge and CH_4 system in the directions that are (a) perpendicular to the water bridge and (b) parallel to the water bridge, $T = 300$ K, $P = 5$ MPa.

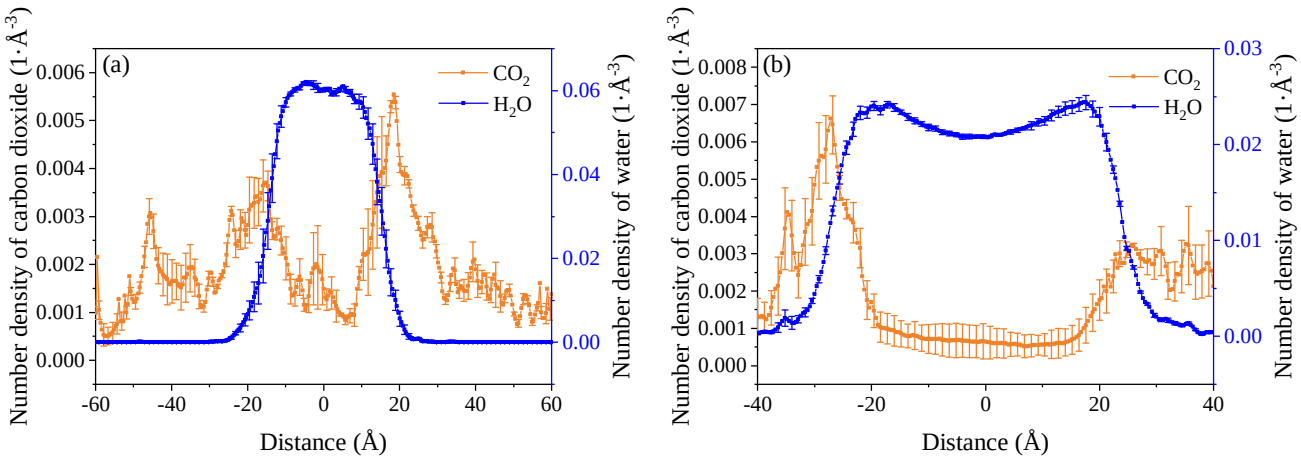

Fig. 3. The density profiles of the water bridge and CO_2 system in the directions that are (a) perpendicular to the water bridge and (b) parallel to the water bridge, $T = 300$ K, $P = 5$ MPa.

to previous studies (Aimoli et al., 2014; Yang et al., 2017; Chong and Myshakin, 2020; Ravipati et al., 2021). CH_4 component shows a random distribution, and it cannot diffuse into the water bridge. In the direction parallel to the water bridge, as shown in Fig. 2(b), H_2O and CH_4 molecules both form the adsorbed layers. CO_2 is also tested on the water bridge system, as shown in Fig. 3, higher density peaks are obtained on the water bridge surface. What is more, CO_2 can diffuse into the H_2O phase, since the oxygen atom of CO_2 can disturb the hydrogen bond structure formed by H_2O molecules (Sadlej et al., 1998; Kumar et al., 2013). In Fig. 3(b), CO_2 presents an extremely strong adsorption capacity, and most CO_2 molecules turn to the adsorbed phase, which will change the surface property of kerogen matrixes, and affects the stability of the water bridge furtherly.

On the base of the water bridge, the pure CH_4 and pure CO_2 components are tested independently. To study the combined effects caused by these two components, the water bridge system, with CH_4 and CO_2, in the kerogen channel is constructed. As shown in Fig. 4(a), the density profiles are similar to the above results, and the CH_4 component has a higher concentration in the channel space, as a result of the stronger adsorption capacity of CO_2. Although distinct results can be obtained in the one-dimensional analyses, the specific reasons and water bridge behaviors are still not clear.

3.2 Density and potential energy in two dimensions

To obtain more information on H_2O and other components, the two-dimensional contours of density and potential energy are counted in the computational domain. There is always a problem that many scholars have discussed, and it is the wettability problem (Hu et al., 2015; Jagadisan and Heidari, 2022; Zhou et al., 2022). Common sense is that H_2O is non-wetting on the organic surface, but the wetting behaviors of H_2O always show the wetting condition on the kerogen surface (Hu et al., 2016; Jagadisan and Heidari, 2019; Zhou et al., 2019b). From the aspect of the model snapshot and one-dimensional analysis, as shown in Fig. 1, the water bridge seems like a wetting phase according to its contact angle.

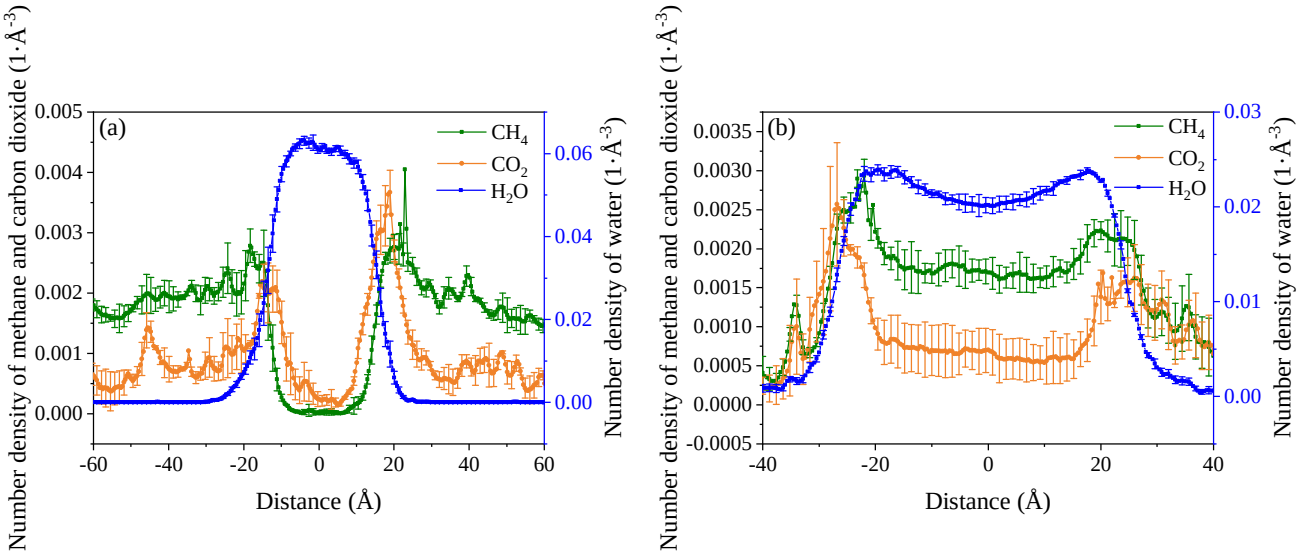

Fig. 4. The density profiles of the water bridge, CH_4, and CO_2 system in the directions that are (a) perpendicular to the water bridge and (b) parallel to the water bridge, $T = 300$ K, $P = 5$ MPa.

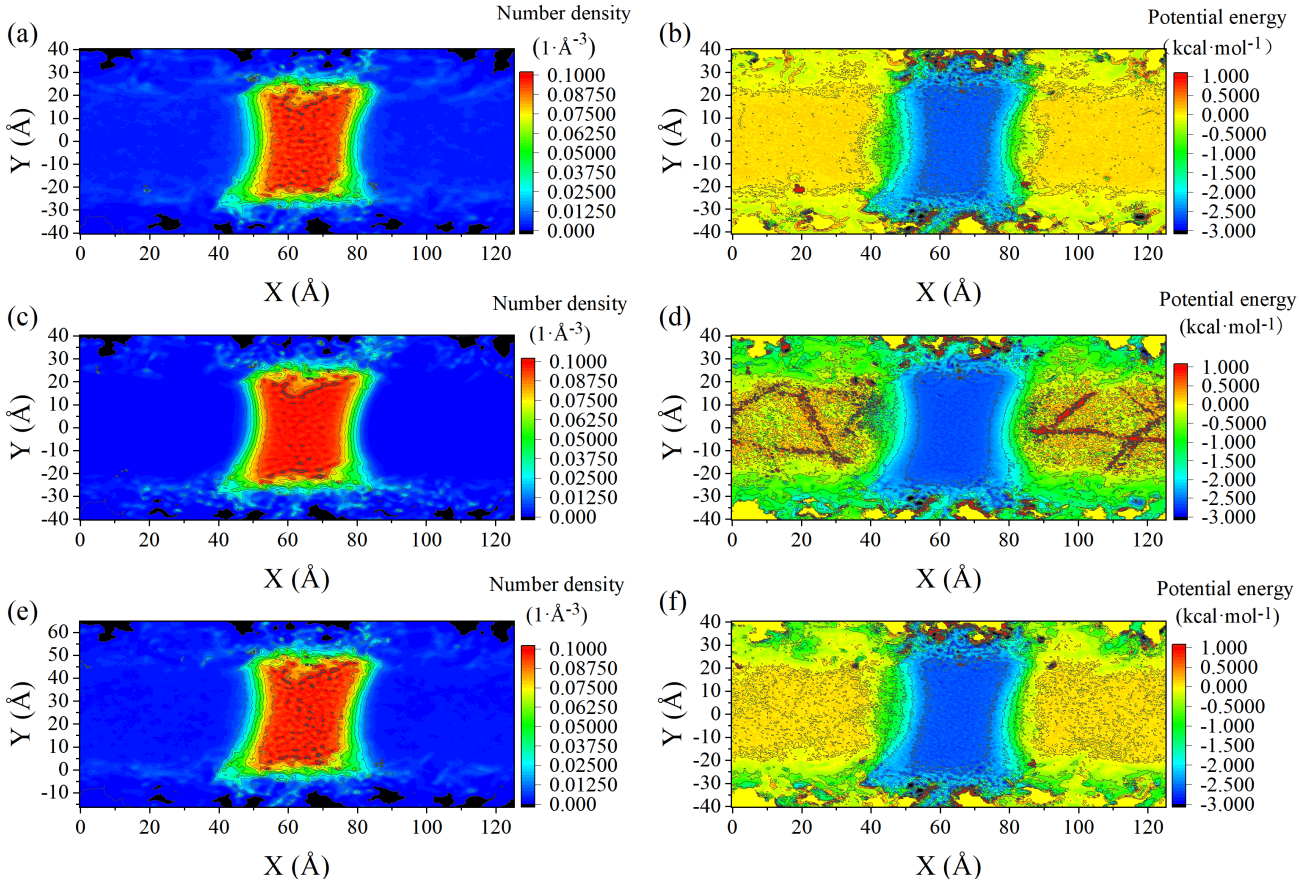

Fig. 5. (a) The density contour, and (b) potential energy contour of water bridge and CH_4 system, (c) the density contour, and (d) potential energy contour of the water bridge and CO_2 system, (e) the density contour, and (f) potential energy contour of the water bridge, CH_4, and CO_2 system. $T = 300$ K, $P = 5$ MPa.

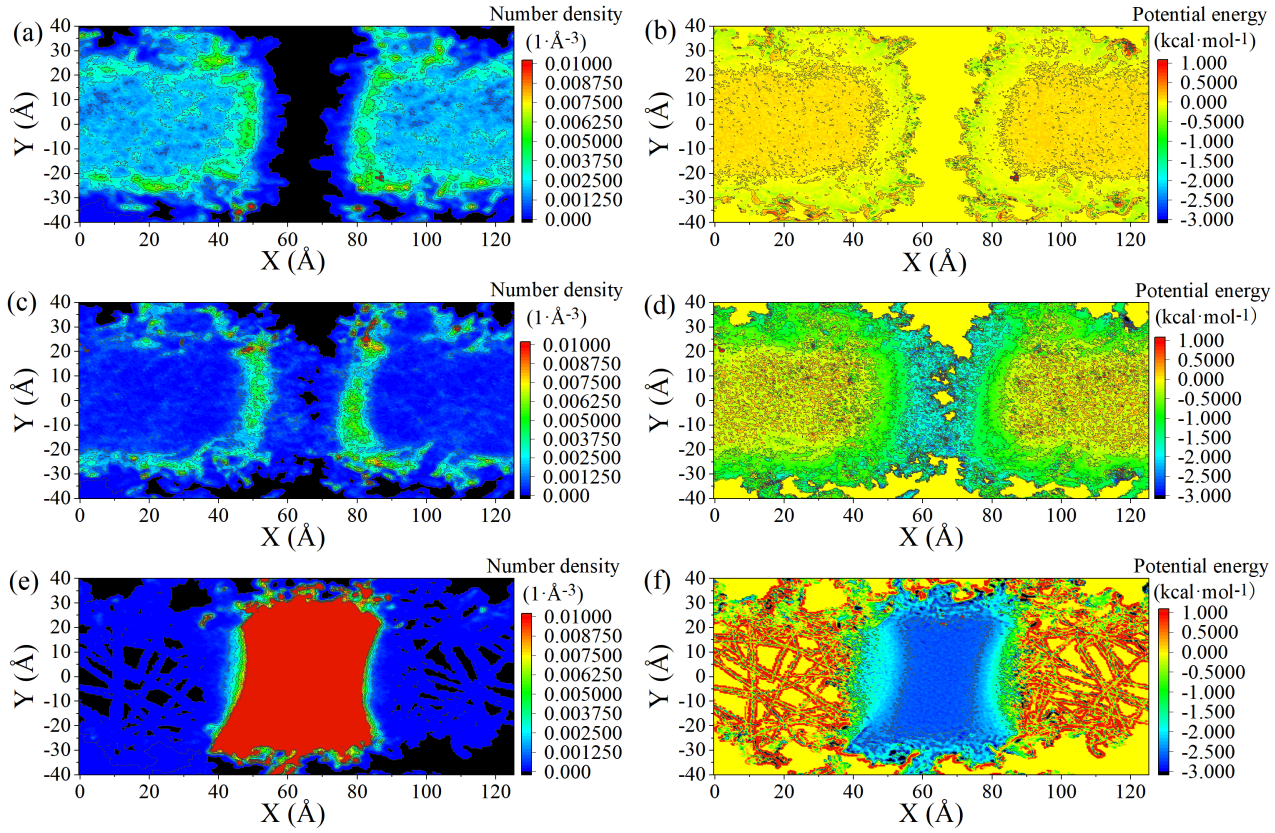

Fig. 6. (a) The density contour, and (b) potential energy contour of the CH_4 component, (c) the density contour, and (d) potential energy contour of the CO_2 component, (e) the density contour, and (f) potential energy contour of the H_2O component. $T = 300$ K, $P = 5$ MPa.

However, Figs. 5(a) and 5(c) present that the main body of the water bridge, i.e., the higher density region, tends to form the non-wetting contact angle. The density declines at the boundary of the H_2O phase, hence the H_2O molecules at the boundary mislead the judgment of the liquid H_2O phase's contact angle. In addition, the diffusion phenomenon can be observed more clearly in this way.

Figs. 5(b) and 5(d) exhibit the potential energy distributions of fluid atoms. The H_2O molecules also diffuse into the kerogen matrix, which is like the roots of trees, suggesting that the water bridge is not easy to be moved with the effect of roots (the hydrogen bond interaction). Therefore, the possible methods to move the water bridge are in two different ways. One way is the change of surface property (Walker et al., 2017; Li et al., 2019), making the water bridge desorb from the kerogen surface, and the second way is made by weakening the interaction between different H_2O molecules. Actually, this is similar to the operations in the development of petroleum (changing the wettability and reducing the viscosity). Obviously, CO_2 has lower potential energy sites on the boundaries of the water bridge and kerogen surfaces, and the low potential energy state caused by CO_2 will facilitate the diffusion of the H_2O phase. The linear high potential energy distribution is generated by some H_2O molecules that steamed from the water bridge. In the water bridge system mixed with CH_4 and CO_2, the result of potential energy contour is an intermediate state in Figs. 5(a)-5(d), suggesting that the CH_4 component will inhibit low potential energy sites.

The results in Fig. 5 are calculated based on the entire fluid molecules, and the specific distributions of each component are not clear, thus the density and potential energy are counted in two-dimensional space for CH_4, CO_2, and H_2O components respectively. Figs. 6(a) and 6(b) present the results of the CH_4 component, where the CH_4 component cannot diffuse into the center of the water bridge, but some CH_4 molecules still can diffuse on the surface of the H_2O phase, because of the weak interaction at the boundary. In addition, the potential energy is zero in the center of the water bridge, and a lower energy layer can be observed on the surface of the water bridge and kerogen matrixes, which is called the adsorbed phase. The bulk phase is in the bulk space except for the adsorbed layer. This is more clearly in the results of CO_2, as shown in Figs. 6(c) and 6(d). CO_2 has a stronger interaction with kerogen and forms denser adsorbed layers. They diffuse into the H_2O phase and have lower potential energy states in the H_2O phase, which also corresponds to previous conclusions (Tenney and Lastoskie, 2006; Yang and Zhong, 2006). Because the water bridge is a liquid phase, the density contour shows a high-density region.

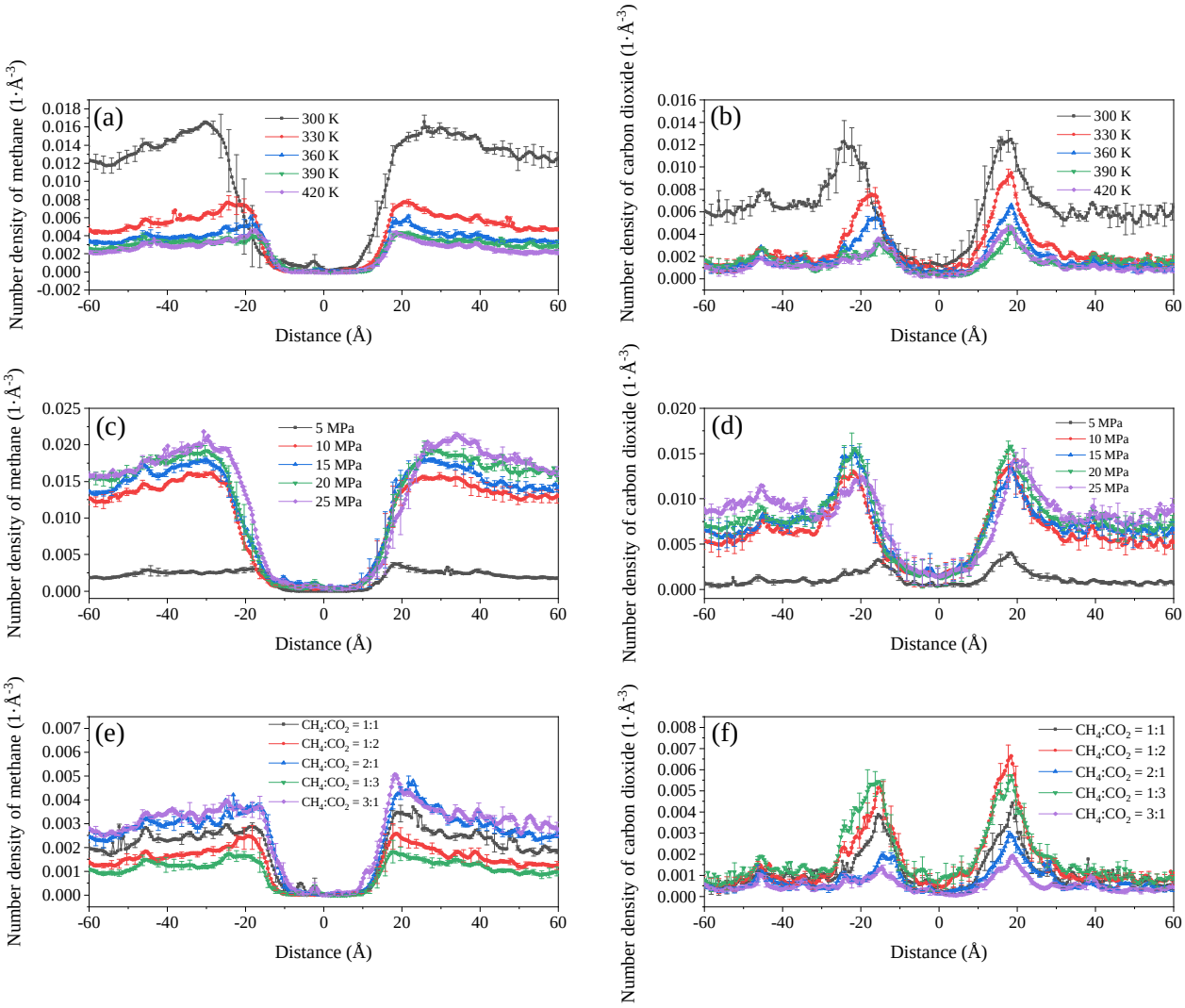

Fig. 7. The density profiles of CH_4 (a) and CO_2 (b) at various temperatures, $P = 10$ MPa, the density profiles of CH_4 (c) and CO_2 (d) at various pressures, $T = 300$ K, the molar ratio of CH_4 and CO_2 in (a-d) is 1:1, the density profiles of CH_4 (e) and CO_2 (f) at various molar ratios. $T = 300$ K, $P = 10$ MPa.

Some H_2O molecules will be free from the liquid phase and diffuse into the bulk phase, because of the molecular thermal motion. These free H_2O molecules form the linear potential distributions in the bulk phase, which is similar to Fig. 5(d). What is more, the lower potential energy is always located in the waist position, since the molecules in the waist have less interaction with kerogen matrixes and more CO_2 molecules. Therefore, CO_2 can weak the stability of the water bridge by diffusing into the H_2O phase, and the most unstable position is in the waist of the water bridge.

3.3 Sensitivity analysis

In addition to the density and potential energy analyses displayed in Figs. 7(a) and 7(b), the effect of temperature on different components is also tested. Obviously, a higher temperature results in a lower density of the gas phase (CH_4 and CO_2) (You et al., 2016). However, at a lower temperature, CO_2 prefers to be liquid phase under certain pressure, the density is higher means the denser adsorbed layer and more instability of the water bridge. As shown in Figs. 7(c) and 7(d), higher pressure means a higher density of gas phase, and CO_2 turns to be liquid state. Thus, in the center of the water bridge, more CO_2 molecules are observed, which reveals that CO_2 can be applied easily in its liquid state. As the shale gas is always a mixture, the varied ratios of CH_4 and CO_2 are examined in Figs. 7(e) and 7(f), and more CO_2 molecules lead to weaker interaction between H_2O molecules, caused by the diffusion of CO_2. When the molar ratio of CH_4 and CO_2 increases to 1:2, a similar result can be obtained in the case of 1:3, hence the 1:2 ratio is a better choice for the low cost of CO_2. In the same way, more CH_4 molecules also facilitate the diffusion on the surface of the H_2O phase, however, it is still on the surface. Therefore, the content of CO_2 is the main role in the stability of the water bridge.

4. Conclusions

In this work, the MD method is utilized to study the stability of the water bridge in the kerogen channel, with the effects of CH_4 and CO_2. CH_4 and CO_2 both tend to form the adsorbed layers on the surfaces of the water bridge and kerogen matrixes, and the CO_2 component prefers to diffuse into the H_2O phase because the hydrogen bonds are disturbed by its molecular polarity. In the two-dimensional analyses, the main body of the H_2O phase is the high-density region, and it shows the non-wetting contact angle, which differs from the results in model visualization and one-dimensional analyses. The adsorbed phase and bulk phase regions are verified according to the potential energy contours. CH_4 can diffuse into the surface of the H_2O phase, and CO_2 diffuses into the bridge center, suggesting that the stability of the water bridge is mainly affected by CO_2 molecules. Higher temperature leads to less content in the gas phase, while CO_2 dissolution of in the H_2O phase is relatively stable. The lower gas density can be generated by higher pressure conditions, and CO_2 turns to be liquid phase accordingly, which enhances the solubility of CO_2 even further. Compared with cases with various molar ratios of CH_4 and CO_2, the molar ratio of 1:2 (CH_4:CO_2) is a better choice. In summary, the stability of water bridge is comprehensively studied in various scenarios, and the potential energy analysis is also carried out to verify the discussions, which provides a better understanding of the development of shale energy, but the phase behaviors of CO_2 are not presented, which is also one of our future research points.

Acknowledgement

We would like to express appreciation to the following financial support: National Natural Scientific Foundation of China (Nos. 51874262 and 51936001), King Abdullah University of Science and Technology (KAUST) through the grants BAS/1/1351-01, URF/1/4074-01, and URF/1/3769-01.

Conflict of interest

The authors declare no competing interest.

Open Access This article is distributed under the terms and conditions of the Creative Commons Attribution (CC BY-NC-ND) license, which permits unrestricted use, distribution, and reproduction in any medium, provided the original work is properly cited.

References

Aimoli, C. G., Maginn, E. J., Abreu, C. R. Transport properties of carbon dioxide and methane from molecular dynamics simulations. The Journal of Chemical Physics, 2014, 141(13): 134101.

An, S., Erfani, H., Hellevang, H., et al. Lattice-boltzmann simulation of dissolution of carbonate rock during CO_2-saturated brine injection. Chemical Engineering Journal, 2021, 408: 127235.

Aspenes, E., Ersland, G., Graue, A., et al. Wetting phase bridges establish capillary continuity across open fractures and increase oil recovery in mixed-wet fractured chalk. Transport in Porous Media, 2008, 74(1): 35-47.

Chong, L., Myshakin, E. M. The effect of residual water content on preferential adsorption in carbon dioxide-methane-illite clay minerals: A molecular simulation study. Fluid Phase Equilibria, 2020, 504: 112333.

Collell, J., Ungerer, P., Galliero, G., et al. Molecular simulation of bulk organic matter in type II shales in the middle of the oil formation window. Energy & Fuels, 2014, 28(12): 7457-7466.

Cui, F., Jin, X., Liu, H., et al. Molecular modeling on gulong shale oil and wettability of reservoir matrix. Capillarity, 2022, 5(4): 65-74.

Feng, Q., Xu, S., Xing, X., et al. Advances and challenges in shale oil development: A critical review. Advances in Geo-Energy Research, 2020, 4(4): 406-418.

Ho, T. A., Striolo, A. Water and methane in shale rocks: Flow pattern effects on fluid transport and pore structure. AIChE Journal, 2015, 61(9): 2993-2999.

Hu, Y., Devegowda, D., Sigal, R. A microscopic characterization of wettability in shale kerogen with varying maturity levels. Journal of Natural Gas Science and Engineering, 2016, 33: 1078-1086.

Hu, Y., Devegowda, D., Striolo, A., et al. Microscopic dynamics of water and hydrocarbon in shale-kerogen pores of potentially mixed wettability. SPE Journal, 2015, 20(1): 112-124.

Huai, J., Xie, Z., Li, Z., et al. Displacement behavior of methane in organic nanochannels in aqueous environment. Capillarity, 2020, 3(4): 56-61.

Humphrey, W., Dalke, A., Schulten, K. VMD: Visual molecular dynamics. Journal of Molecular Graphics, 1996, 14(1): 33-38.

Hunt, J. M., Jamieson, G. W. Oil and organic matter in source rocks of petroleum. AAPG Bulletin, 1956, 40(3): 477-488.

Jagadisan, A., Heidari, Z. Demystifying wettability alteration in kerogen as a function of its geochemistry and reservoir temperature and pressure using molecular dynamics simulations. Paper SPE 195863 Presented at SPE annual technical conference and exhibition, Calgary, Alberta, Canada, 30 September-2 October, 2019.

Jagadisan, A., Heidari, Z. Molecular dynamic simulation of the impact of thermal maturity and reservoir temperature on the contact angle and wettability of kerogen. Fuel, 2022, 309: 122039.

Javadpour, F. Nanopores and apparent permeability of gas flow in mudrocks (shales and siltstone). Journal of Canadian Petroleum Technology, 2009, 48(8): 16-21.

Kadoura, A., Narayanan Nair, A. K., Sun, S. Molecular dynamics simulations of carbon dioxide, methane, and their mixture in montmorillonite clay hydrates. The Journal of Physical Chemistry C, 2016, 120(23): 12517-12529.

Kumar, A., Sakpal, T., Linga, P., et al. Influence of contact medium and surfactants on carbon dioxide clathrate hydrate kinetics. Fuel, 2013, 105: 664-671.

Li, T., Li, J., Lin, H., et al. Control of wettability transition and coalescence dynamics of droplets on the surface via mechanical vibration: A molecular simulation exploration. Applied Surface Science, 2019, 473: 393-400.

Liu, B., Liu, W., Pan, Z., et al. Supercritical CO_2 breaking through a water bridge and enhancing shale oil recovery: A molecular dynamics simulation study. Energy & Fuels, 2022a, 36(14): 7558-7568.

Liu, J., Xie, X., Meng, Q., et al. Effects of membrane structure on oil-water separation by smoothed particle hydrodynamics. Membranes, 2022b, 12(4): 387.

Liu, H., Xiong, H., Yu, H., et al. Effect of water behaviour on the oil transport in illite nanopores: Insights from a molecular dynamics study. Journal of Molecular Liquids, 2022c, 354: 118854.

Liu, J., Yang, Y., Sun, S., et al. Flow behaviors of shale oil in kerogen slit by molecular dynamics simulation. Chemical Engineering Journal, 2022d, 434: 134682.

Liu, P., Zhang, T., Sun, S. A tutorial review of reactive transport modeling and risk assessment for geologic CO_2 sequestration. Computers & Geosciences, 2019, 127: 1-11.

Liu, J., Zhao, Y., Yang, Y., et al. Multicomponent shale oil flow in real kerogen structures via molecular dynamic simulation. Energies, 2020, 13(15): 3815.

Perez, F, Devegowda, D. Spatial distribution of reservoir fluids in mature kerogen using molecular simulations. Fuel, 2019, 235: 448-459.

Ravipati, S., Santos, M. S., Economou, I. G., et al. Monte carlo molecular simulation study of carbon dioxide sequestration into dry and wet calcite pores containing methane. Energy & Fuels, 2021, 35(14): 11393-11402.

Rexer, T. F., Mathia, E. J., Aplin, A. C., et al. High-pressure methane adsorption and characterization of pores in posidonia shales and isolated kerogens. Energy & Fuels, 2014, 28(5): 2886-2901.

Sadlej, J., Makarewicz, J., Chałasiński, G. Ab initio study of energy, structure and dynamics of the water-carbon dioxide complex. The Journal of chemical physics, 1998, 109(10): 3919-3927.

Shen, W., Li, X., Cihan, A., et al. Experimental and numerical simulation of water adsorption and diffusion in shale gas reservoir rocks. Advances in Geo-Energy Research, 2019, 3(2): 165-174.

Srinivasan, S. G., Ashok, I., Jônsson, H., et al. Parallel short-range molecular dynamics using the ādhāra runtime system. Computer Physics Communications, 1997, 102(1-3): 28-43.

Tenney, C. M., Lastoskie, C. M. Molecular simulation of carbon dioxide adsorption in chemically and structurally heterogeneous porous carbons. Environmental Progress, 2006, 25(4): 343-354.

Tesson, S., Firoozabadi, A. Methane adsorption and self-diffusion in shale kerogen and slit nanopores by molecular simulations. The Journal of Physical Chemistry C, 2018, 122(41): 23528-23542.

Ungerer, P., Collell, J., Yiannourakou, M. Molecular modeling of the volumetric and thermodynamic properties of kerogen: Influence of organic type and maturity. Energy & Fuels, 2015, 29(1): 91-105.

Waldman, M., Hagler, A. T. New combining rules for rare gas van der waals parameters. Journal of Computational Chemistry, 1993, 14(9): 1077-1084.

Walker, S. M., Marcano, M. C., Kim, S., et al. Understanding calcite wettability alteration through surface potential measurements and molecular simulations. The Journal of Physical Chemistry C, 2017, 121(50): 28017-28030.

Yang, Y., Li, Y., Yao, J., et al. Dynamic pore-scale dissolution by CO_2-saturated brine in carbonates: Impact of homogeneous versus fractured versus vuggy pore structure. Water Resources Research, 2020a, 56(4): e2019WR026112.

Yang, Y., Liu, J., Yao, J., et al. Adsorption behaviors of shale oil in kerogen slit by molecular simulation. Chemical Engineering Journal, 2020b, 387: 124054.

Yang, Y., Narayanan Nair, A. K., Sun, S. Molecular dynamics simulation study of carbon dioxide, methane, and their mixture in the presence of brine. The Journal of Physical Chemistry B, 2017, 121(41): 9688-9698.

Yang, Y., Narayanan Nair, A. K., Sun, S. Adsorption and diffusion of carbon dioxide, methane, and their mixture in carbon nanotubes in the presence of water. The Journal of Physical Chemistry C, 2020c, 124(30): 16478-16487.

Yang, Q., Zhong, C. Molecular simulation of carbon dioxide/methane/hydrogen mixture adsorption in metal-organic frameworks. The Journal of Physical Chemistry B, 2006, 110(36): 17776-17783.

York, D. M., Darden, T. A., Pedersen, L. G. The effect of long-range electrostatic interactions in simulations of macromolecular crystals: A comparison of the ewald and truncated list methods. Journal of Chemical Physics, 1993, 99(10): 8345-8348.

You, J., Tian, L., Zhang, C., et al. Adsorption behavior of carbon dioxide and methane in bituminous coal: A molecular simulation study. Chinese Journal of Chemical Engineering, 2016, 24(9): 1275-1282.

Zhang, J., Li, X., Zou, X., et al. Characterization of the full-sized pore structure of coal-bearing shales and its effect on shale gas content. Energy & Fuels, 2019, 33(3): 1969-1982.

Zhang, M., Zhan, S., Jin, Z. Recovery mechanisms of hydrocarbon mixtures in organic and inorganic nanopores during pressure drawdown and CO_2 injection from molecular perspectives. Chemical Engineering Journal, 2020, 382: 122808.

Zhao, J., Ren, L., Jiang, T., et al. Ten years of gas shale fracturing in china: Review and prospect. Natural Gas Industry B, 2022, 9(2): 158-175.

Zhou, J., Hu, N., Xian, X., et al. Supercritical CO_2 fracking for enhanced shale gas recovery and CO_2 sequestration: Results, status and future challenges. Advances in Geo-Energy Research, 2019a, 3(2): 207-224.

Zhou, J., Mao, Q., Luo, K. H. Effects of moisture and salinity on methane adsorption in kerogen: A molecular simulation study. Energy & Fuels, 2019b, 33(6): 5368-5376.

Zhou, J., Zhang, J., Yang, J., et al. Mechanisms for kerogen wettability transition from water-wet to CO_2-wet: Implications for CO_2 sequestration. Chemical Engineering Journal 2022, 428: 132020.